Northumbria Research Link

Northumbria
University
NEWCASTLE

University Library

CrossMark

ORIGINAL ARTICLE

A microstructural insight into the hygro-mechanical behaviour of a stabilised hypercompacted earth

Agostino Walter Bruno · **Céline Perlot** · **Joao Mendes** · **Domenico Gallipoli**

Abstract The use of raw earth as construction material can save embodied and operational energy because of low processing costs and passive regulation of indoor ambient conditions. Raw earth must however be mechanically and/or chemically stabilised to enhance stiffness, strength and water durability. In this work, stiffness and strength are enhanced by compacting raw earth to very high pressures up to 100 MPa while water durability is improved by using alkaline solutions and silicon based admixtures. The effect of these stabilisation methods on hygro-mechanical behaviour is explored and interpreted in terms of the microstructural features of the material. Stiffness and strength are defined at different humidity levels by unconfined compression tests while the moisture buffering capacity is measured by humidification/desiccation cycles as prescribed by the norm ISO 24353 (Hygrothermal performance of building materials and products determination of moisture adsorption/desorption properties in response to humidity variation. International Organization for Standardization, Geneva, 2008). As for the microstructural characterisation, different tests (i.e. X-ray diffractometry, Infrared Spectroscopy, Mercury Intrusion Porosimetry, Nitrogen Adsorption) are performed to analyse the effect of stabilisation on material fabric and mineralogy. Results indicate that the use of alkaline activators and silicon based admixtures significantly improves water durability while preserving good mechanical and moisture buffering properties. Similarly, the compaction to very high pressures results in high levels of stiffness and strength, which are comparable to those of standard masonry bricks. This macroscopic behaviour is then linked to the microscopic observations to clarify the mechanisms through which stabilisation affects the properties of raw earth at different scales.

A. W. Bruno (✉) · C. Perlot · D. Gallipoli
Laboratoire SIAME - Bâtiment ISABTP, Fédération IPRA, EA4581, Université de Pau et des Pays de l'Adour, Allée du Parc Montaury, 64600 Anglet, France
e-mail: agostinowalter.bruno@univ-pau.fr

J. Mendes
Department of Mechanical and Civil Engineering, Northumbria University, Newcastle upon Tyne, UK

1 Introduction

The use of raw earth as a construction material for load-bearing, infilling or partition walls can reduce environmental impact during both the construction and service life of buildings. Raw earth can be locally sourced and, when suitably manufactured in the form

rilem

of blocks or panels, it exhibits excellent mechanical properties at significantly lower costs than conventional building materials [2, 3]. Moreover, during service life, raw earth walls can passively regulate both indoor humidity, thanks to their high moisture buffering capacity, and temperature, through exchanges of latent heat, thus increasing environmental comfort for occupants while reducing air-conditioning needs [4–8].

Despite the above advantages, dissemination of raw earth into mainstream construction practice has so far been hindered by economic and processing difficulties linked to soil selection, speed of construction and labour costs [9]. Additional obstacles have been posed by technical limitations associated to the relatively poor levels of stiffness, strength and water durability of this material. To improve mechanical and durability properties, raw earth is often "stabilised" by either mechanical processes, e.g. through densification, or chemical processes, e.g. through mineral cementation. Some methods are more effective in improving stiffness and strength but less effective in enhancing durability, while other methods exhibit opposite results. As pointed out by Liuzzi et al. [10] and McGregor et al. [11], some stabilisation methods can also induce undesirable side effects like a reduction of the material hygro-thermal inertia, defined as the ability of the material to store/release heat and moisture depending on the temperature and relative humidity of the surrounding environment.

A relatively large number of studies have investigated mechanical stabilisation of raw earth showing that densification through compaction improves significantly mechanical and durability performance [12–16]. This is also consistent with earlier studies on conventional fired bricks, which have shown a strong dependency of durability on the pore size distribution of the material [17–22].

Other studies have instead privileged chemical stabilisation to improve the durability of raw earth [23–30]. Unfortunately, chemical stabilisation tends to produce a noticeable reduction of moisture buffering capacity and limits the ability of the material to passively regulate indoor temperature and humidity [11].

Chemical stabilisation by means of alkaline additives, instead of conventional hydraulic binders such as cement and lime, can contribute to the reduction of embodied energy. Alkaline activation relies on an increase of the pH to trigger the release of silicon and aluminium ions naturally present in clays and the subsequent cationic exchange with calcium ions from the cementitious phase. This cationic exchange has two consequences: (1) the precipitation of silicon and aluminium hydrates [31] and (2) the flocculation of clay platelets induced by a change of the electrostatic double layer. The above reactions, which occur more effectively at an optimum pH of 12.4 [32], can be catalysed by different alkaline activators such as potassium or sodium hydroxide and potassium or sodium silicate [33, 34]. Another recently proposed chemical stabilisation method involves the application of waterproofing agents such as silicone admixtures either on the surface of the finished walls or inside the earth prior to compaction. These agents react with the soil substrate forming a hydrophobic polysiloxane film inside the material capillaries, which increases resistance to water erosion [35]. This favourable effect is however partly undermined by a reduction of moisture buffering capacity and vapour permeability [36].

The present work investigates the influence of mechanical and chemical stabilisation on the hygro-mechanical properties and, in particular, on the stiffness, strength and moisture buffering capacity of raw earth. Mechanical stabilisation is performed by densification through compaction at relatively large pressures from 25 to 100 MPa. Chemical stabilisation is instead achieved by mixing the earth with different liquid additives such as alkaline solutions and silicon hydro-repellent admixtures. Among the various alkaline activators, sodium hydroxide has been chosen in this study because of its efficiency in improving mechanical performance while maintaining good material hygroscopicity [37–39]. In the sake of simplicity and for consistency with previous terminology, we will use the term "unstabilised" to indicate compacted samples made of just earth and water while we will use the term "stabilised" to indicate compacted samples made of earth and liquid additives.

Stiffness and strength have been determined by means of uniaxial compression tests after equalisation at different humidity levels while moisture buffering capacity has been measured by cycles of relative humidity at constant temperature according to the norm ISO 24353 [1].

In general, the material enhancement produced by mechanical or chemical stabilisation is linked to a significant modification of microstructural characteristics

such as a change of pore size distribution, porosity, density and specific surface. Therefore, an extensive campaign of microstructural tests, including X-ray diffractometry, Infrared Spectroscopy, Mercury Intrusion Porosimetry and Nitrogen Adsorption Porosimetry, has been performed in the present work to understand the effect of mechanical and chemical stabilisations on material fabric. The results from this microstructural characterisation provide unprecedented insight into the mechanisms through which stabilisation affects the mechanical and moisture buffering behaviour of the tested materials.

2 Materials and methods

The earth used in the present work has been provided by a brickwork factory from the region of Toulouse in the south-west of France. Figure 1 shows the grain size distribution of the tested material together with the boundaries that delimit the admissible region according to manufacturing guidelines for compressed earth bricks, i.e. MOPT [40], CRATerre-EAG [41] and AFNOR [42]. Inspection of Fig. 1 indicates that the grain size distribution of the tested earth lies close to the finest boundary of the admissible region. As observed by Jaquin et al. [43] and Beckett and Augarde [44], finer soils are able to retain more water than coarser ones when exposed to the same hygro-

thermal conditions, thus resulting in stronger hygroscopic behaviour.

The plasticity properties of the fine fraction, i.e. the fraction passing through 400 μm, were measured according to the norm NF P94-051 [45]. The liquid limit is 33.0% while the plasticity index is 12.9%, which correspond to an inorganic clay of medium plasticity according to the Unified Soil Classification System [46]. These properties comply with existing recommendations for the manufacture of compressed earth bricks [41, 42, 47]. The activity of the fine fraction, i.e. the ratio between plasticity index and clay fraction, is equal to 0.79, which corresponds to a normally active material [48]. This is also consistent with the mineralogical composition observed during X-ray diffraction tests, which indicated a predominantly illitic material with a small quantity of montmorillonite. Illite is a three-layers clay with good bonding characteristics and limited swelling upon wetting, which makes it suitable for raw earth construction [49].

Cylindrical samples of 50 mm diameter and 100 mm high were produced by static compaction of earth at pressures up to 100 MPa inside a thick steel mould. This sample preparation method has been termed "hypercompaction" due to the relatively large magnitude of the applied pressure. Prior to compaction, the dry soil was mixed with pure water (in the case of unstabilised samples) or with a liquid additive (in the case of stabilised samples) for at least 15 min

Fig. 1 Grain size distribution of tested earth
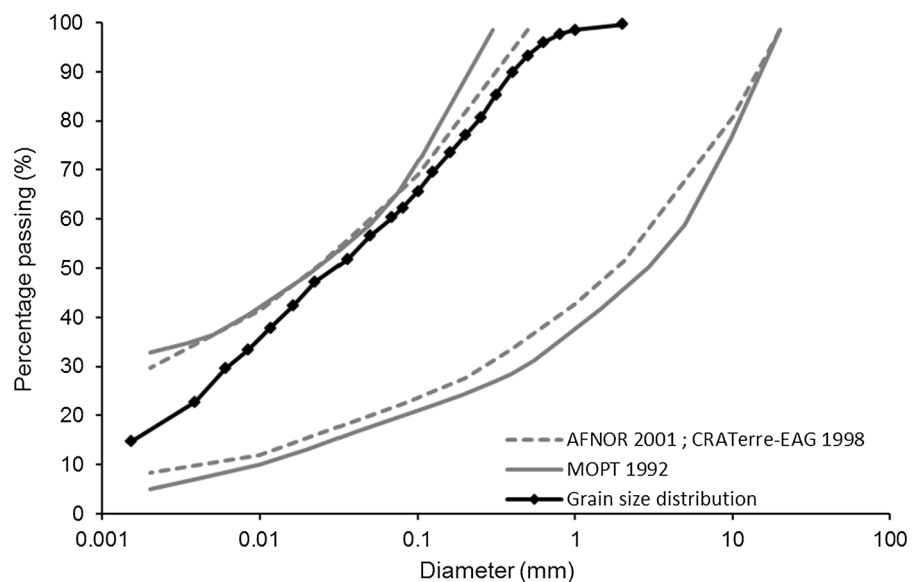
by using a planetary mixer. After mixing, the soil was compacted inside a "floating" mould with two pistons at bottom and top extremities as shown in Fig. 2. This double-compaction reduced the effect of friction between the earth and the mould surface, thus increasing stress uniformity and fabric homogeneity across the sample height. Results from Mercury Intrusion Porosimetry tests on small specimens taken at different sample heights confirmed the good homogeneity of the material [50]. This hypercompaction method resulted in a very dense material with a minimum porosity of 15% for the highest pressure of 100 MPa. Further details about the sample preparation method can be found in Bruno [50].

Unstabilised samples were compacted at three pressure levels of 25, 50 and 100 MPa with water contents of 8.1, 6.2 and 5.2%, respectively. These three water contents correspond to the optimum values determined from the compaction curves for each pressure level [50]. Stabilised samples were instead only compacted at the highest pressure of 100 MPa after replacing the 5.2% water content of the unstabilised samples with an equal amount of liquid additive. The application of the highest compaction pressure of 100 MPa also to the stabilised samples was necessary to enable a homogeneous comparison between different materials and to explore the effect of chemical stabilisation on the samples with the best

possible characteristics. The liquid additives chosen in this work consisted in a blend of silane-siloxane emulsion (commercial name GPE50P from Tech-Dry) and sodium hydroxide solution. The very small amount of stabilising additive is expected not to increase significantly the environmental impact of the material, though further analysis in this respect is necessary.

To define the exact additive formulation, a number of preliminary immersion tests were performed on samples stabilised with silane-siloxane emulsions of different concentrations and sodium hydroxide solutions of different molarities [51]. The immersion tests were performed according to the German norm DIN 18945 [52] by dipping samples of the stabilised earth for ten minutes in water and by measuring the corresponding mass loss. Based on the observed results, the following three stabilising additives were selected for further testing due to their good performance [51]:

- 5.2% NaOH solution at 2 mol/l concentration—mass loss of 5.64%
- 1.08% silane-siloxane emulsion + 4.12% NaOH solution at 2 mol/l concentration—mass loss of 4.18%
- 5.2% silane-siloxane emulsion—mass loss of 1.36%

Fig. 2 Schematic and photograph of compaction set-up
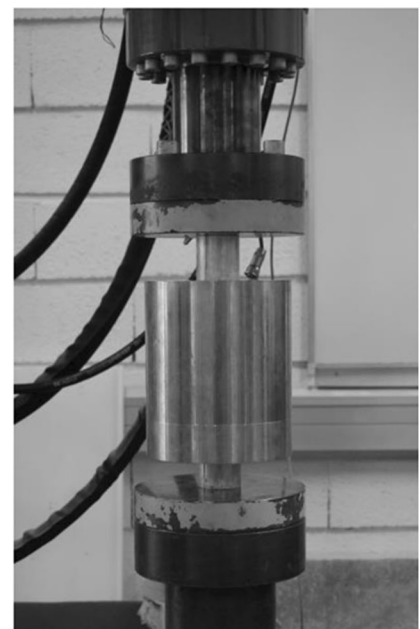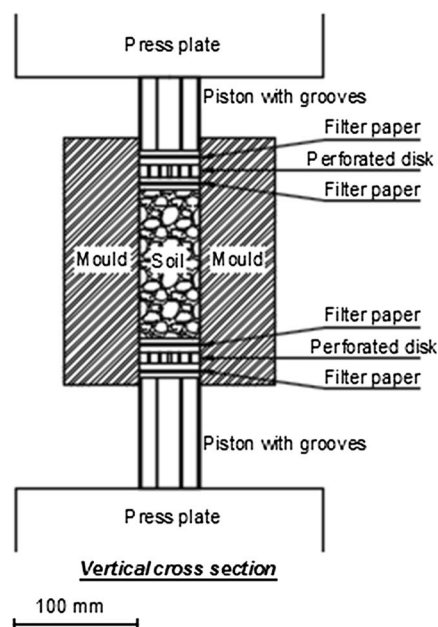
The viscosity of the NaOH solution is similar to that of pure water, which means that the rheology of the NaOH stabilised earth is the same as that of the unstabilised earth. This generates an identical dry density of 2275 kg/m^3 for these two types of samples after compaction. Conversely, the silane-siloxane emulsion is not soluble and exhibits a slightly higher viscosity than pure water, which reduces the dry density of the silane-siloxane stabilised samples of about 1% compared to the unstabilised ones.

3 Microstructural characterisation

Mercury Intrusion Porosimetry (MIP) tests were performed to investigate the density, pore size distribution and specific surface area of both unstabilised and stabilised samples. These microstructural properties have a strong influence on the mechanical and moisture buffering behaviour of earthen materials. Small sample fragments of about 2 cm^3 were equalised for 1 week inside a climatic chamber to the same temperature of 25 °C and relative humidity of 62% to eliminate any influence of ambient conditions. After equalisation, the specimens were freeze-dried to remove pore water by causing minimal disturbance to the material fabric. The freeze-drying process consisted in rapidly freezing the specimens by immersion in liquid nitrogen ($T = -196$ °C) until boiling ended. This was followed by sublimation of ice under vacuum at a temperature of -50 °C for at least 2 days. The dried specimens were then introduced in a penetrometer, which was inserted inside the low pressure chamber (compressed air chamber) of the MIP device. Prior to mercury intrusion, the gas pressure was lowered to 50 µmHg for 5 min to evacuate all air and any residual moisture from the soil pores. Mercury was then intruded into the material under increasing pressures from 10 to 200 kPa, which correspond to the penetration of the larger pore diameters from 10^5–10^4 nm. After this, the penetrometer was transferred to the high pressure chamber (compressed oil chamber) where the pressure of mercury was further increased to 200 MPa to detect the smaller pore diameters down to 10^1 nm. After completion of the intrusion path, the pressure of mercury was decreased back to 360 kPa to measure the extrusion path.

Nitrogen Adsorption (NA) tests were also performed to investigate the very small pore range down to 2 nm. Specimens of about 0.5 cm^3 (around 1 g) were equalised for 1 week at a temperature of 25 °C and a relative humidity of 62% before being freeze-dried likewise in MIP tests. The specimens were subsequently inserted inside a penetrometer connected to the NA device where they were subjected to one nitrogen intrusion-extrusion cycle at a constant temperature of 77 K (-196 °C). This cycle consisted in the pressurisation of gaseous nitrogen up to the saturation value of 1 atm (absolute) followed by depressurisation back to the initial value. Throughout the cycle, the amount of intruded nitrogen was continuously measured to determine the isothermal adsorption and desorption curves, which were then processed to determine the pore size distribution according to the Barrett–Joyner–Halenda BJH model [53].

Figure 3 shows the three pore size distributions measured during MIP tests on unstabilised samples compacted to 25, 50 and 100 MPa, respectively. Inspection of Fig. 3 indicates that the porosity, n reduces from 19 to 15% as the compaction pressure increases from 25 to 100 MPa. The pore diameter that separates the region of the large inter-aggregate pores from the region of the small intra-aggregate pores was defined at 50 nm by comparing cumulative extrusion and intrusion curves according to the method suggested by Tarantino and De Col [54]. Interestingly, Fig. 3 shows that the inter-aggregate porosity (i.e. the volume of the pores with diameter larger than 50 nm) reduces significantly with increasing compaction effort. Conversely, the influence of compaction effort on the intra-aggregate porosity (i.e. the volume of pores with diameter smaller than 50 nm) is very limited. This is important because the stiffness and strength of raw earth are strongly affected by inter-aggregate porosity and are therefore also significantly influenced by compaction effort. Conversely, compaction effort has no influence on the hygroscopic behaviour, which is controlled by intra-aggregate porosity. This hypothesis is confirmed by the results from the hygro-mechanical tests presented in the next section.

The effect of compaction effort on intra-aggregate porosity, i.e. the porosity smaller than 50 nm, was further investigated by Nitrogen Adsorption tests. Results from these tests are shown in Fig. 4, which

Fig. 3 MIP tests. Pore size distributions of unstabilised samples compacted at 25, 50 and 100 MPa
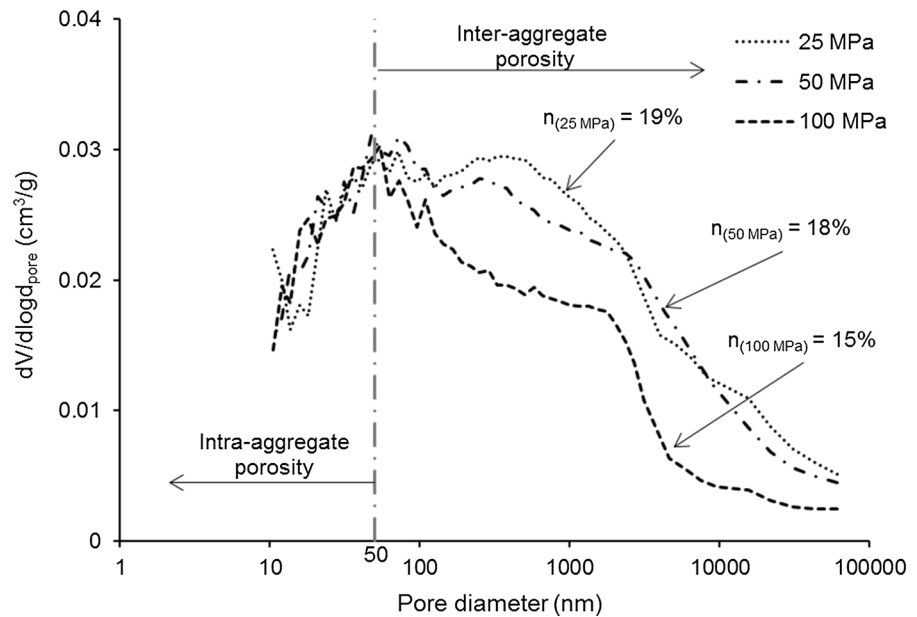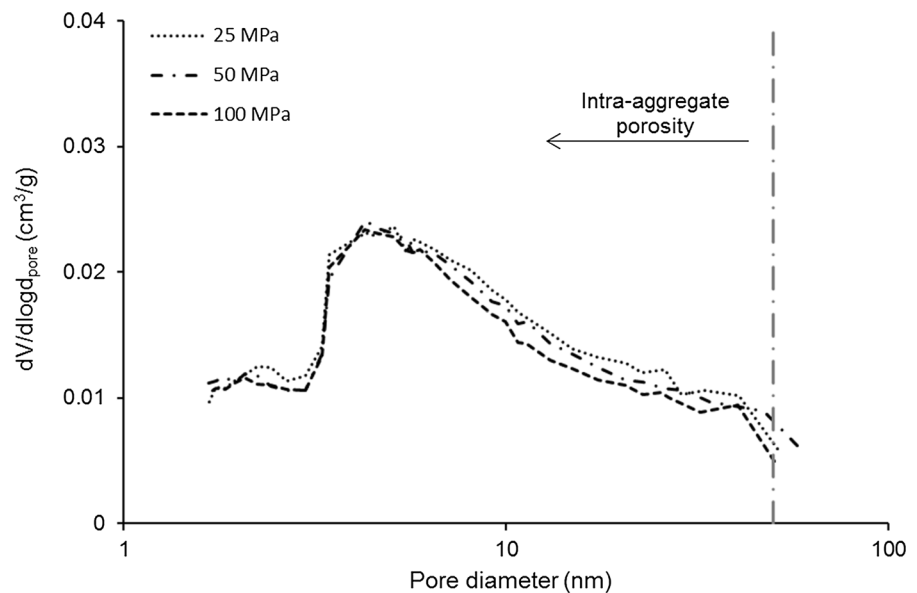

Fig. 4 Nitrogen Adsorption tests. Pore size distributions of unstabilised samples compacted at 25, 50 and 100 MPa

indicates that the pore size distributions of the samples compacted at 25, 50 and 100 MPa overlap over the entire pore range, thus confirming the results previously obtained from MIP tests.

Additional MIP and NA tests were carried out to investigate the influence of chemical stabilisation on material fabric. Figure 5 compares the pore size distributions from MIP tests on unstabilised and stabilised samples compacted at 100 MPa. Stabilisation creates a new class of inter-aggregate pores,

which was absent in unstabilised samples, with a diameter comprised between 10^4 and 10^5 nm. This might be due to the steric hindrance of stabilisers molecules between clay platelets. This new class of pores reduces the stiffness and strength of stabilised samples compared to unstabilised ones as discussed later in the paper.

Stabilisation also occludes the smallest nanoporous fraction and therefore modifies the intra-aggregate porosity distribution. This is shown in Fig. 6, where
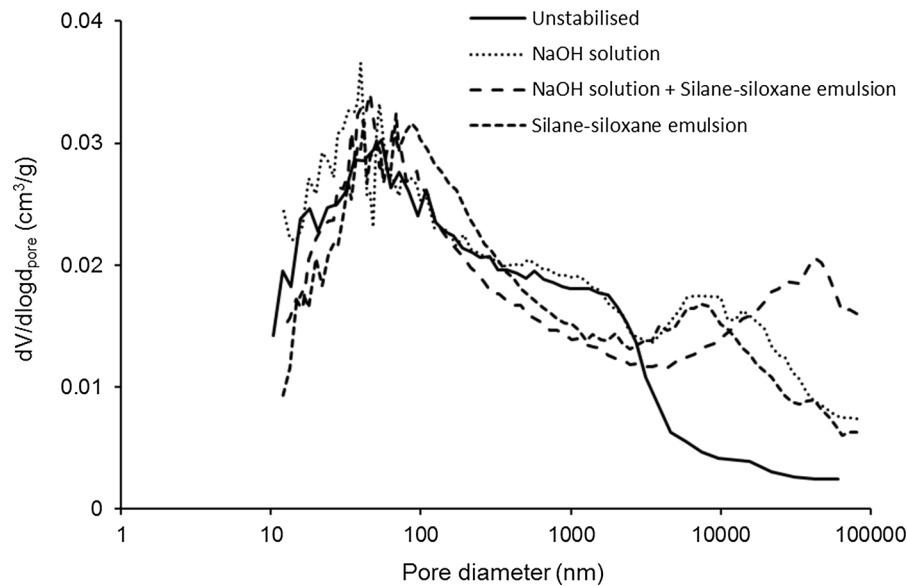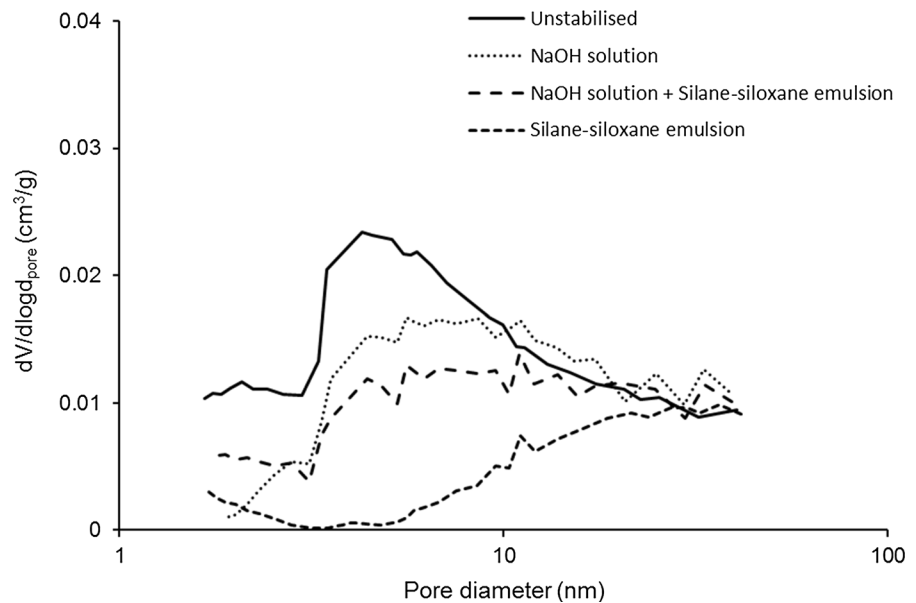
Fig. 5 MIP tests. Pore size distributions of unstabilised and stabilised samples compacted at 100 MPa

Fig. 6 Nitrogen Adsorption tests. Pore size distributions of unstabilised and stabilised samples compacted at 100 MPa

results from NA tests indicate that the silane-siloxane emulsion produces the largest nanopore occlusion due to the formation of a polysiloxane hydrophobic film inside the earth capillaries. The occlusion of nanopores significantly undermines the ability of the material to buffer moisture as discussed in the following section. Interestingly, both unstabilised and stabilised samples exhibit a similar overall porosity of about 15% [50], which means that any

difference in hygro-mechanical behaviour between these two classes of samples is rather due to variations in the distribution of pore sizes and mineralogy.

To investigate how the mineralogical composition of raw earth is affected by chemical stabilisation, X-ray Diffractometry (XRD) and Infrared Spectroscopy (IS) tests were performed on pulverised specimens obtained by grinding cylindrical samples. XRD tests made use of a Cu X-ray source emitting

radiation at 1.54 Å wavelength and a generator operating at 30 kV and 10 mA. The crystalline phases of the material were detected by simultaneously rotating both the X-rays source and receptor with a total angle to the horizontal of 2θ, where θ is the angle between the X-rays source (or the receptor) and the horizontal. Preliminary tests were conducted by varying the angle 2θ from $5°$ to $90°$ and with a 1 mm wide beam. The range of the angle 2θ was then restricted to $2°$–$15°$ and the beam enlarged to 2 mm at a slower scan rate to better visualise the argillite minerals. Figure 7 shows the results from these tests and indicates that, as expected, the silane-siloxane emulsion does not form any new crystalline phase. Conversely, the NaOH solution generates a cementing zeolite phase, which is a crystalline aluminosilicate with tetrahedral sites produced by alkaline activation of the clay fraction, as also observed by Van Jaarsveld et al. [55].

To further investigate the nature of chemical bonds within crystalline structures, Infrared Spectroscopy (IS) tests were performed on both unstabilised and stabilised samples compacted at 100 MPa by recording spectra between 550 and 4000 cm^{-1}. Figure 8 shows that the samples stabilised with the NaOH solution exhibit the highest reduction of transmittance at a characteristic vibrational band corresponding to a wavelength of 1040 cm^{-1}, thus indicating the formation of more intense Si–O–Si bonds compared to other

samples. The 690 and 580 cm^{-1} bands are instead associated with Al–O stretching vibrations of condensed octahedral AlO$_6$ and, also in this case, the NaOH stabilised samples showed the largest reduction of transmittance. This is due to the fact that the clay matrix undergoes dehydroxylation in an alkaline environment, which changes the aluminium coordination from octahedral to tetrahedral corresponding to the formation of zeolite as already observed from XRD tests. The high transmittance of the silane-siloxane stabilised samples at 1040 cm^{-1} and between 690 and 580 cm^{-1} suggests that this stabilisation generates fewer bonds between silica and aluminium oxides compared with NaOH stabilised samples. Moreover, the decrease of the transmittance at about 3000 cm^{-1} exhibited by the silane-siloxane stabilised samples indicates a weakening stretch of the methylene and methyl C–H bonds, as also observed by Innocenzi and Brusatin [56]. This further confirms the weaker bonding capacity of the silane-siloxane emulsion compared with the NaOH solution.

4 Mechanical and hygroscopic characterisation

4.1 Stiffness and strength

The effect of ambient humidity on stiffness and strength was measured by means of unconfined

Fig. 7 Diffractograms from XRD tests on unstabilised and stabilised samples compacted at 100 MPa
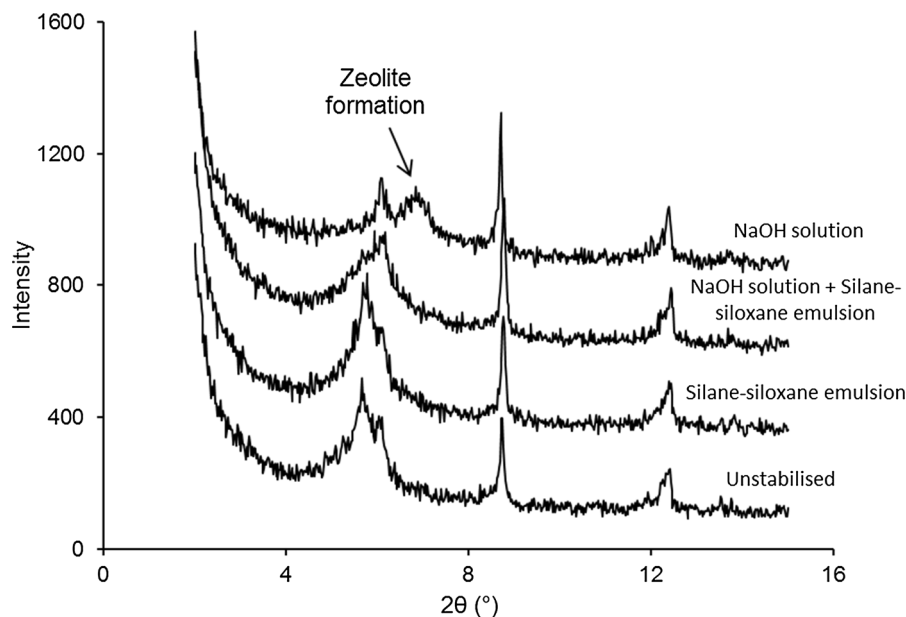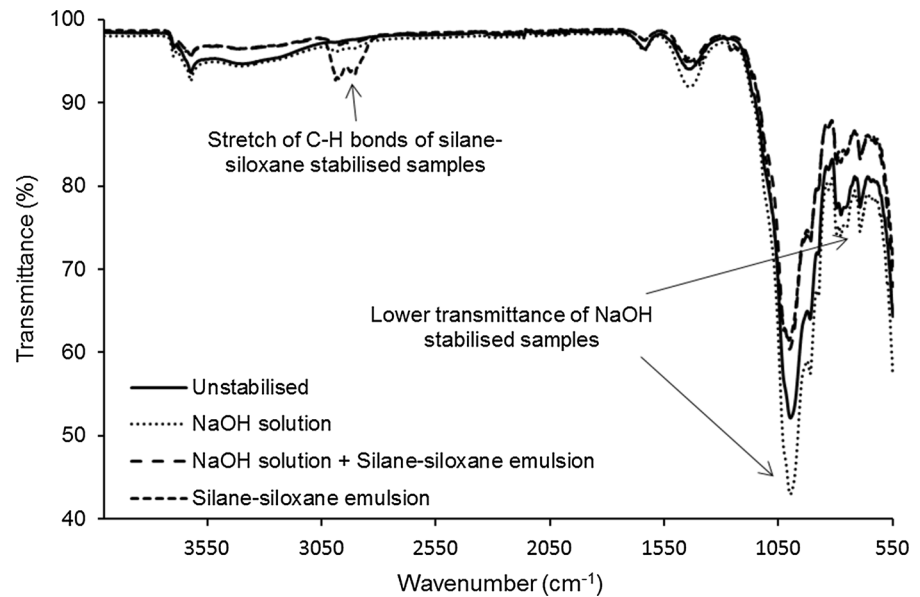
Fig. 8 Infrared spectra of unstabilised and stabilised samples compacted at 100 MPa

compression tests on unstabilised and stabilised cylindrical samples. Prior to testing, the samples were equalised at a constant temperature of 25 °C and five different relative humidities of 25, 44, 62, 77 and 95%. Equalisation was considered complete when the sample mass became constant, which took typically 2 weeks.

During testing, relative axial displacements were recorded between two points at a distance of 50 mm along the height of the sample by means of two extensometers located on diametrically opposite sides. The axial strain was then calculated from the average of these two measurements. To determine the Young modulus, the samples were subjected to five cycles of loading–unloading at a rate of 5 kPa/s between one-ninth and one-third of the ultimate material strength. The ultimate material strength was estimated as the average of the peak load measured during two preliminary compression tests. The Young modulus was then calculated as the average slope of the best fit lines of the five unloading stress–strain curves [51]. This procedure is based on the assumption that material behaviour is markedly elasto-plastic during loading but approximately elastic during unloading. After the fifth loading–unloading cycle, all samples were loaded until failure with a constant displacement rate of 0.001 mm/s to measure the post-peak region of the stress–strain curve. Spurious confinement due to friction between the sample ends and the loading

plates was minimised by applying Teflon spray on the top and bottom press plates before placing them in contact with the sample faces.

Figures 9 and 10 show the variation of both Young modulus and compressive strength with relative humidity for the unstabilised samples compacted at 25, 50 and 100 MPa. These results indicate that hypercompaction significantly improves the stiffness and strength of raw earth at all levels of relative humidity. This increase of stiffness and strength with growing compaction effort is associated to a change of pore size distribution, as shown Figs. 3 and 4, and in particular to a marked reduction of the inter-aggregate porosity larger than 50 nm. The measured values of Young modulus and compressive strength are one order of magnitude higher than those reported in previous studies on rammed earth materials (e.g. [57]). They are also comparable with those of traditional construction materials such as standard masonry bricks or cement-stabilised earth [58].

Figures 9 and 10 also show that growing ambient humidity induces a marked deterioration of mechanical characteristics. This is because an increase of ambient humidity reduces capillary tension inside the pores, which is the primary source of stiffness and strength in unstabilised earth materials (e.g. [59–61]).

Figures 11 and 12 show the variation of Young modulus and compressive strength with relative humidity for the stabilised samples compacted at
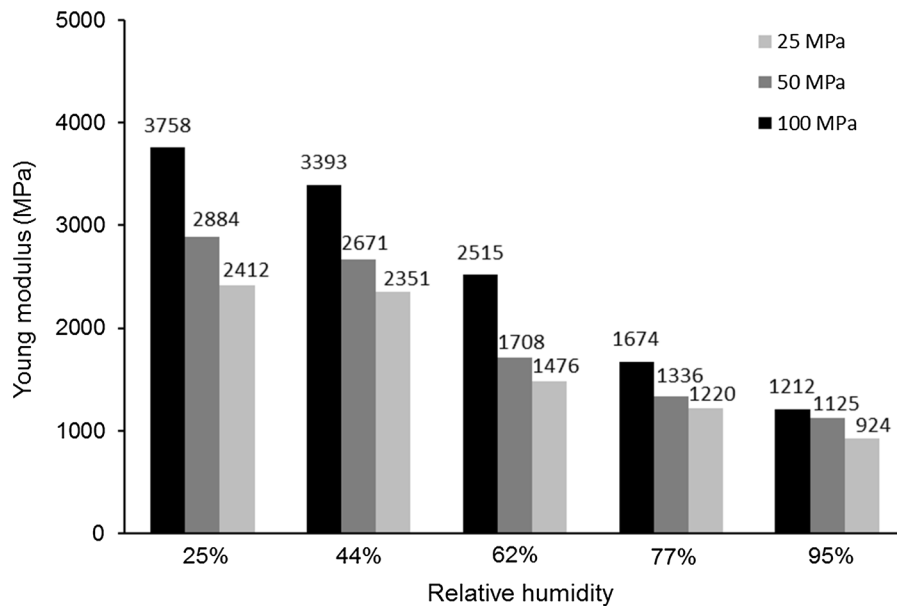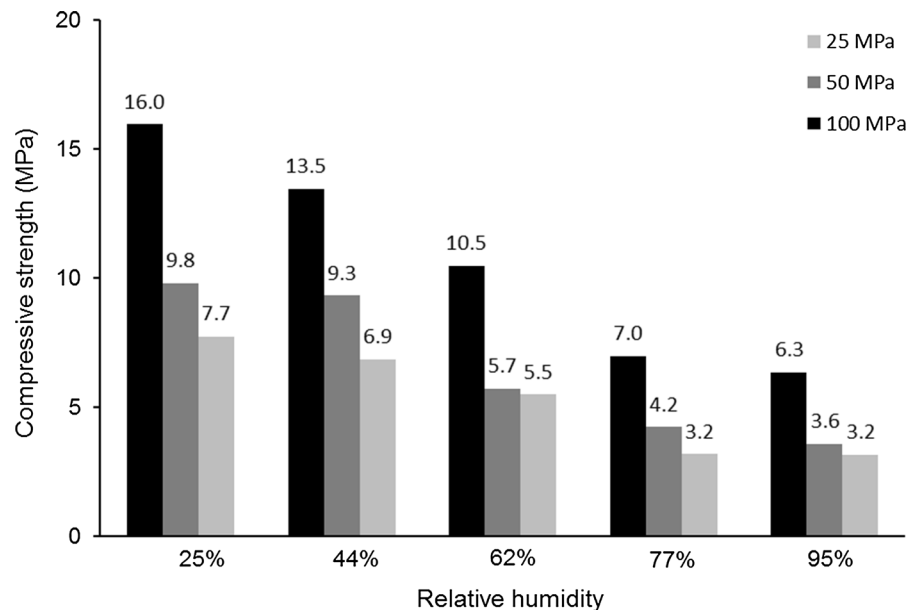
Fig. 9 Variation of Young modulus with relative humidity: unstabilised samples compacted at 25, 50 and 100 MPa

Fig. 10 Variation of compressive strength with relative humidity: unstabilised samples compacted at 25, 50 and 100 MPa

100 MPa. The Young modulus and compressive strength of the unstabilised samples compacted at 100 MPa are also reported in the same figure for ease of comparison. Perhaps surprisingly, stabilised samples exhibit lower levels of stiffness and strength compared to the unstabilised ones. This is explained by the fact that the stabilisation methods considered in this study produce an additional class of larger inter-

aggregate pores that does not exist in the unstabilised material. This new class of larger inter-aggregates pores includes diameters comprised between 10^4 and 10^5 nm (Fig. 5).

Among all stabilised samples, only those prepared with the NaOH solution exhibit values of stiffness and strength that are comparable to those of unstabilised ones. The good mechanical characteristics of the

Fig. 11 Variation of Young modulus with relative humidity: unstabilised and stabilised samples compacted at 100 MPa
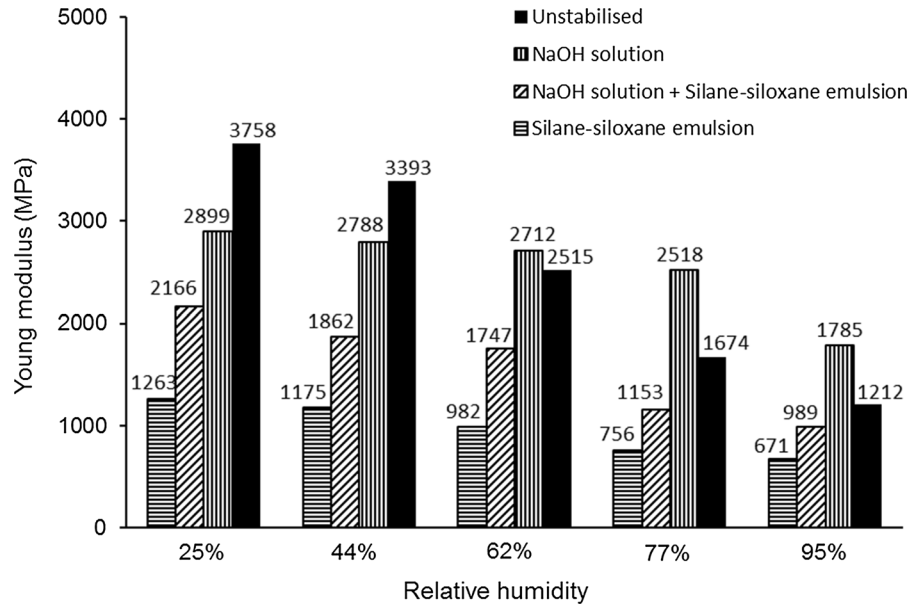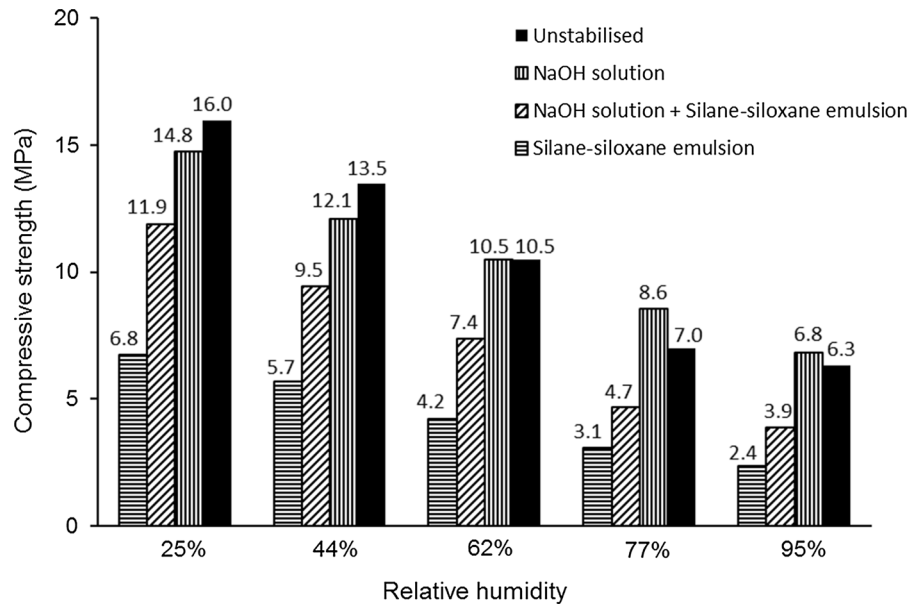

Fig. 12 Variation of compressive strength with relative humidity: unstabilised and stabilised samples compacted at 100 MPa

samples stabilised with the NaOH solution are probably due to the formation of a cementing zeolite fraction as observed from X-ray diffraction tests (Fig. 7) and Infrared Spectroscopy tests (Fig. 8). This cementing zeolite fraction is not visible in the samples stabilised with the silane-siloxane emulsion, whose X-ray diffractogram is very similar to that of the unstabilised samples (Fig. 7). On the contrary, the silane-siloxane emulsion deteriorates mechanical performance due to the formation of a new class of inter-

aggregate pores (Fig. 5) caused by the steric hindrance of stabilisers molecules. The silane-siloxane emulsion also produces fewer bonds between silica and aluminium oxides while causing a stretch of the methylene and methyl C–H bonds as observed from Infrared Spectroscopy tests (Fig. 8).

Figures 11 and 12 show that stabilised samples exhibit decreasing levels of strength and stiffness with increasing ambient humidity, which is similar to unstabilised samples. Nevertheless, stabilisation with

the NaOH solution significantly reduces the sensitivity of mechanical properties to ambient humidity in comparison to all other materials. In particular, as the relative humidity increases from 25 to 95%, the NaOH stabilised samples exhibit a reduction of compressive strength of 54% compared to 61% for the unstabilised samples, 65% for the silane-siloxane stabilised samples and 67% for the samples stabilised with both NaOH solution and silane-siloxane emulsion. A similar trend can also be observed for the reduction of Young modulus with increasing relative humidity.

4.2 Moisture buffering capacity

Raw earth exhibits an excellent capacity to buffer ambient humidity due to its elevated specific surface and extended network of nanopores [62]. The dependency of material hygroscopicity on the finest pores with diameters of only few nanometers can be shown by combining the Kelvin law and Young–Laplace equation for the idealised case of cylindrical pores with zero contact angle. The imposed values of temperature T and relative humidity RH can then be converted into an equivalent pore diameter d_{pore}:

$$d_{pore} = -\frac{4\gamma V_m}{RT \ln\left(\frac{RH}{100}\right)} \qquad (1)$$

where γ is the surface tension of water (72.3 mN/m at 23 °C), V_m is the molar volume of water (18.06 cm^3/mol at 23 °C) and R is the universal gas constant (8.314 J/mol K). The value d_{pore} calculated by Eq. (1) corresponds to the diameter of the pore where condensation and evaporation of water will spontaneously occur during a wetting and drying path, respectively, at a temperature T and a relative humidity RH. For example, a cyclic variation of relative humidity between 53 and 75% at a temperature of 23 °C, as imposed during moisture buffering tests according to the norm ISO 24353 [1], will induce repeated condensation and evaporation of water inside pore diameters comprised between 3 and 7 nm. Of course, Eq. (1) only provides a rough estimation of pore diameter and more complex models, accounting for the thickness of the adsorbed water layer (e.g. the BJH method by [53]) but also for the hysteretic nature of retention mechanisms, should be used to obtain better predictions. Nevertheless, the degree of

approximation achieved with Eq. (1) is considered acceptable for the scope of the present paper. High hygroscopicity is also associated to elevated thermal inertia as water evaporation and condensation generate storage and release of latent heat. This further reinforces the importance of the pore size distribution of construction materials in passively controlling hygro-thermal conditions inside dwellings.

Mechanical and chemical stabilisation can modify the pore size distribution of earth materials (Figs. 5 and 6) and can therefore influence moisture buffering capacity. To investigate this aspect, the moisture buffering value (MBV) of both unstabilised and stabilised earth compacted to 100 MPa was measured according to the norm ISO 24353 [1] by exposing cylindrical samples to cycles of ambient humidity. The cycles took place inside a climatic chamber between the two relative humidity levels of 53 and 75%, with each level maintained for a period of 12 h. During cycles, the temperature was fixed at 25 °C, which is consistent with the equalisation temperature adopted during mechanical tests but slightly higher than the 23 °C prescribed by the norm ISO 24353 [1]. This small difference in temperature should, however, not have any major effect on the measured MBV as observed by Künzel [63].

Prior to the humidity cycles, all samples were equalised at a temperature of 25 °C and a relative humidity of 53% until attainment of a constant mass, which typically occurred after a period of 2 weeks. Five cycles of relative humidity were then performed, which was sufficient to attain steady state conditions corresponding to the measurement of three consecutive "stable cycles" as prescribed the norm ISO 24353 [1]. A stable cycle is defined as a cycle where moisture uptake at a humidity of 75% is equal to moisture release at a humidity of 53%. Samples masses were recorded periodically during testing by means of a scale with a resolution of 0.01 g.

Results from MBV tests are typically presented in terms of moisture adsorption curves, where moisture adsorption is the ratio between the sample mass change (i.e. the difference between the current and initial mass) and the sample area exposed to the ambient humidity. In this work, moisture adsorption curves were determined for each material as the average of three replica tests.

Figure 13 shows the moisture adsorption curve of the last stable cycle for unstabilised samples

Fig. 13 Moisture adsorption of unstabilised samples compacted at 25, 50 and 100 MPa
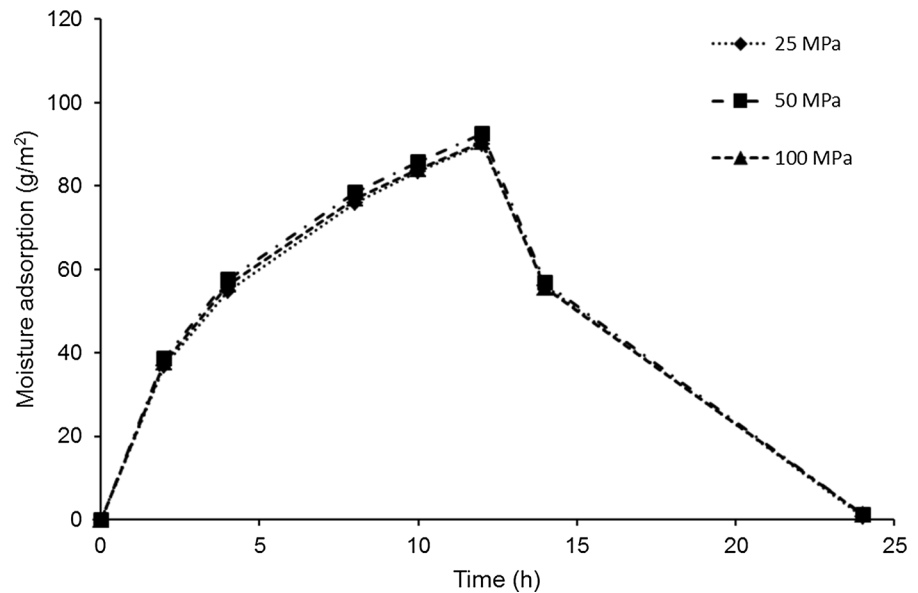
compacted at 25, 50 and 100 MPa, which indicates that the material exhibits a virtually identical moisture buffering capacity regardless of compaction level. This is because exchanges of water vapour take place within the smallest nanoporous fraction, with diameters between 3 and 7 nm, which is not affected by compaction (Fig. 4).

Unstabilised samples compacted at 25, 50 and 100 MPa exhibit however different inter-aggregate porosities, i.e. different amounts of pores with diameters larger than 50 nm (Fig. 3), which is expected to have an effect on the vapour permeability of the samples. The consequence of this difference on the moisture buffering response appears however negligible (Fig. 13), which suggests that only the superficial sample layer, which is less affected by vapour permeability, contributes to the moisture exchanges with the surrounding environment.

Figure 14 shows the moisture adsorption curve corresponding to the last stable cycle of unstabilised and stabilised samples compacted at 100 MPa. Inspection of Fig. 14 indicates that stabilisation reduces the moisture buffering capacity of the material and that the magnitude of this reduction is dependent on the type of stabiliser. The samples stabilised with the NaOH solution show a higher moisture buffering capacity than the samples stabilised with the silane-siloxane emulsion. Samples stabilised with a mix of both NaOH solution and silane-siloxane emulsion

exhibit an intermediate behaviour between the above two. This reduction of moisture buffering capacity is due to the partial occlusion of nanopores produced by the chemical stabilisers as observed during NA tests (Fig. 6).

The moisture buffering value (MBV) of both unstabilised and stabilised samples was calculated by using the following standard equation:

$$\text{MBV} = \frac{\Delta m}{S\,\Delta\%\text{RH}} \qquad (2)$$

where Δm is the variation of sample mass in grams induced by the change in relative humidity over the last three stable cycles, S is the exposed surface in square meters and $\Delta\%$ RH is the percentage difference between the extremes of the relative humidity cycle.

For each material, the average MBV measured during uptake and release of moisture over the last three stables cycles is plotted in Fig. 15 together with the classification proposed by Rode et al. [64]. Note that this classification is based on a different testing procedure where relative humidity ranges between 33 and 75% with asymmetric steps of 16 and 8 h, respectively. Due to these differences in testing procedures and the non-linearity of the sorption–desorption curves, the comparison between the MBVs measured in the present work and the classification proposed by Rode et al. [64] can only provide a qualitative assessment of the moisture buffering capacity of the tested materials.

Fig. 14 Moisture adsorption of unstabilised and stabilised samples compacted at 100 MPa
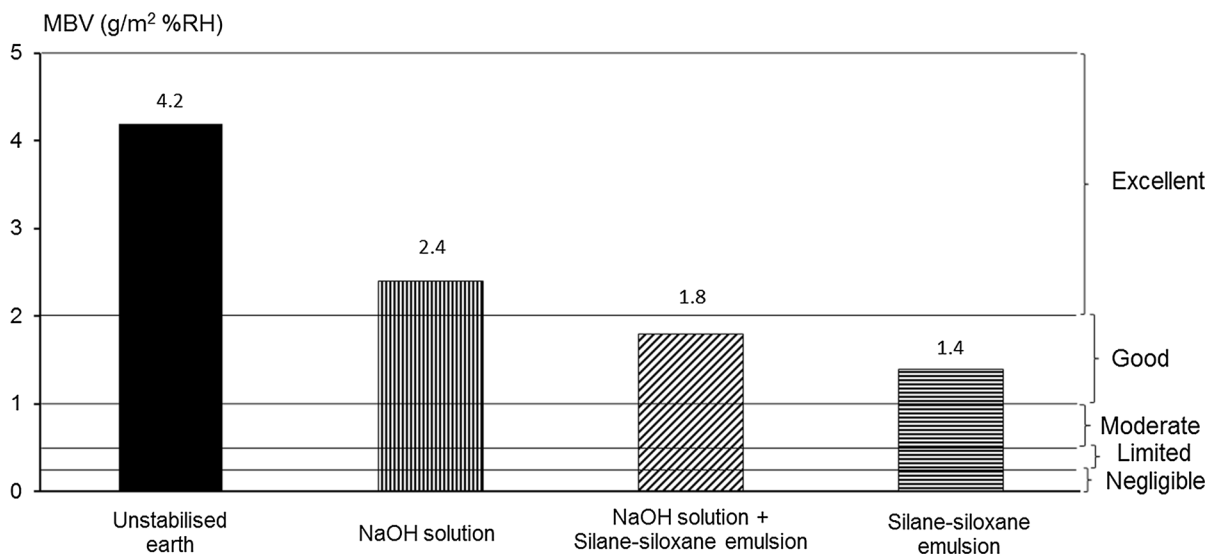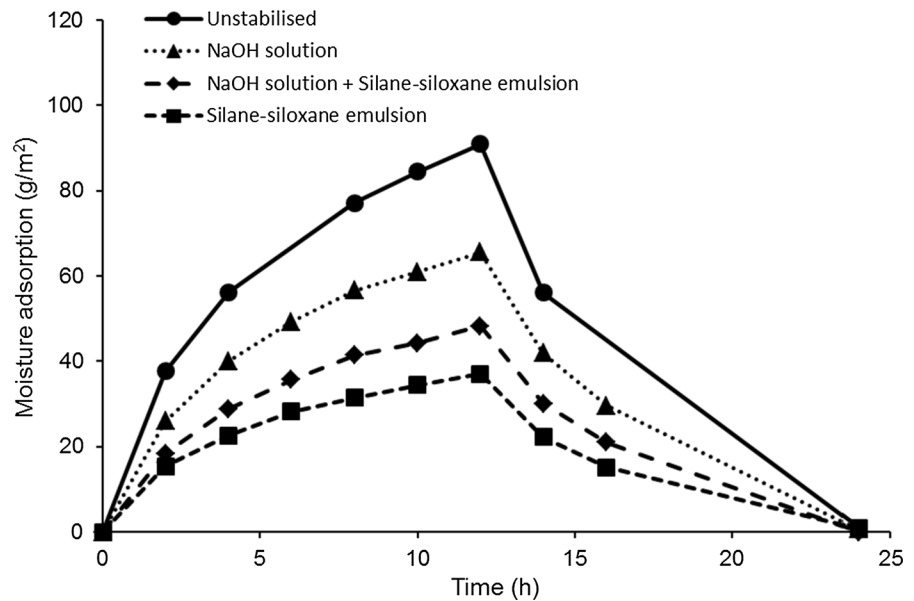

Fig. 15 MBV of unstabilised and stabilised samples compacted at 100 MPa

Figure 15 confirms once again that stabilisation reduces moisture buffering capacity, though the MBV of the material stabilised with the NaOH solution is still excellent while the MBV of the other two stabilised materials is relatively good.

5 Conclusions

The present work investigates the hygro-mechanical behaviour of raw earth focusing on the effect of mechanical and chemical stabilisation on the characteristics of the material measured at different scales. At microscopic level, the study concentrates on the measurement of the pore size distribution and mineralogy while, at macroscopic level, the study focuses on the determination of stiffness, strength and moisture

buffering capacity. The main outcomes of the work can be summarised as follows:

- Compaction at very large pressures improves remarkably the stiffness and strength of raw earth. Conversely, the moisture buffering capacity remains virtually unchanged regardless of compaction effort.
- An increase of compaction effort from 25 to 100 MPa leads to a twofold augmentation of strength and to a significant increase of stiffness at all humidity levels. This corresponds to a considerable reduction of inter-aggregate porosity with a negligible variation of intra-aggregate porosity with increasing compaction effort.
- Stabilisation by NaOH solutions and silane-siloxane emulsions enhances water durability but deteriorates moisture buffering characteristics. This is probably caused by the partial occlusion of the finest pore fraction, with diameters smaller than 50 nm, which is the most effective fraction in storing and releasing water.
- Chemical stabilisation induces a rather surprising reduction of stiffness and strength compared to the unstabilised case. This might be due to the formation of a new class of inter-aggregate pores with a diameter between 10^4 and 10^5 nm, which does not exist in the unstabilised samples.
- Samples stabilised with the silane-siloxane emulsion exhibit the highest water durability but also the largest deterioration of mechanical and moisture buffering properties compared to the other unstabilised samples. The deterioration of mechanical performance is produced by the existence of fewer bonds between silica and aluminium oxides but also by the stretch of the methylene and methyl C–H groups. The decline of retention performance is instead the consequence of the deposition of a thin hydrophobic layer over the earth capillaries.
- Samples stabilised with the NaOH solution exhibit slightly worse water durability than samples stabilised with the silane–siloxane emulsion. Conversely, they exhibit the best mechanical and moisture buffering properties among all stabilised samples. This is due to formation of an additional zeolitic cementing fraction and to the preservation of a largely unconstrained nanopore fraction.

- An increase of ambient humidity produces a reduction of stiffness and strength in both unstabilised and stabilised samples. However, the sensitivity to humidity appears significantly reduced in samples stabilised with the NaOH solution.

Compliance with ethical standards

References

1. ISO 24353 (2008) Hygrothermal performance of building materials and products determination of moisture adsorption/desorption properties in response to humidity variation. International Organization for Standardization, Geneva
2. Deboucha S, Hashim R (2011) A review on bricks and stabilized compressed earth blocks. Scientific Research and Essays 6(3):499–506
3. Morel JC, Mesbah A, Oggero M, Walker P (2001) Building houses with local materials: means to drastically reduce the environmental impact of construction. Build Environ 36(10):1119–1126
4. Allinson D, Hall M (2010) Hygrothermal analysis of a stabilised rammed earth test building in the UK. Energy Build 42(6):845–852
5. Gallipoli D, Bruno AW, Perlot C, Mendes J (2017) A geotechnical perspective of raw earth building. Acta Geotech 12:1–16

6. Pacheco-Torgal F, Jalali S (2012) Earth construction: lessons from the past for future eco-efficient construction. Constr Build Mater 29:512–519

7. Soudani L, Fabbri A, Morel JC, Woloszyn M, Chabriac PA, Wong H, Grillet AC (2016) Assessment of the validity of some common assumptions in hygrothermal modeling of earth based materials. Energy Build 116:498–511

8. Soudani L, Woloszyn M, Fabbri A, Morel JC, Grillet AC (2017) Energy evaluation of rammed earth walls using long term in situ measurements. Sol Energy 141:70–80

9. Easton D (2007) The rammed earth house. Chelsea Green Publishing, Hartford

10. Liuzzi S, Hall MR, Stefanizzi P, Casey SP (2013) Hygrothermal behaviour and relative humidity buffering of unfired and hydrated lime-stabilised clay composites in a Mediterranean climate. Build Environ 61:82–92

11. McGregor F, Heath A, Fodde E, Shea A (2014) Conditions affecting the moisture buffering measurement performed on compressed earth blocks. Build Environ 75:11–18

12. Attom MF (1997) The effect of compactive energy level on some soil properties. Appl Clay Sci 12(1):61–72

13. Kouakou CH, Morel JC (2009) Strength and elasto-plastic properties of non-industrial building materials manufactured with clay as a natural binder. Appl Clay Sci 44(1):27–34

14. Mesbah A, Morel JC, Olivier M (1999) Clayey soil behaviour under static compaction test. Mater Struct 32(223):687–694

15. Olivier M, Mesbah A (1986) Le matériau terre: Essai de compactage statique pour la fabrication de briques de terre compressées. Bull. Liaison Lab. Ponts et Chaussées 146:37–43

16. Venkatarama Reddy BV, Jagadish KS (1993) The static compaction of soils. Geotechnique 43(2)

17. Crooks RW, Kilgour CL, Winslow DN (1986) Pore structure and durability of bricks. In: Proceedings of 4th Canadian masonry symposium (2nd edn.), 1 Department of Civil Engineering, The University of New Brunswick, Fredericton NB, Canada (2–4 June 1986), pp 314–323

18. Haynes JM, Sneck T (1972) Pore properties in the evaluation of material. In: Performance concept in buildings. Proceedings of a joint symposium held in Philadelphia, May 2–5, 1972. National bureau of standards, pp 669–675

19. Maage M (1984) Frost resistance and pore size distribution in bricks. Matériaux et Construction 17(5):345–350

20. Robinson GC (1984) The relationship between pore structure and durability of brick. Am Ceram Soc Bull 63(2):295–300

21. Winslow D (1991) Predicting the durability of paving bricks. J Test Eval 19(1):29–33

22. Winslow DN, Kilgour CL, Crooks RW (1988) Predicting the durability of bricks. J Test Eval 16(6):527–531

23. Bahar R, Benazzoug M, Kenai S (2004) Performance of compacted cement-stabilised soil. Cement Concr Compos 26(7):811–820

24. Guettala A, Abibsi A, Houari H (2006) Durability study of stabilized earth concrete under both laboratory and climatic conditions exposure. Constr Build Mater 20(3):119–127

25. Jayasinghe C, Kamaladasa N (2007) Compressive strength characteristics of cement stabilized rammed earth walls. Constr Build Mater 21(11):1971–1976

26. Khadka B, Shakya M (2016) Comparative compressive strength of stabilized and un-stabilized rammed earth. Mater Struct 49(9):3945–3955

27. Miqueleiz L, Ramírez F, Seco A, Nidzam RM, Kinuthia JM, Tair AA, Garcia R (2012) The use of stabilised Spanish clay soil for sustainable construction materials. Eng Geol 133:9–15

28. Nagaraj HB, Sravan MV, Arun TG, Jagadish KS (2014) Role of lime with cement in long-term strength of compressed stabilized earth blocks. Int J Sustain Built Environ 3(1):54–61

29. Venkatarama Reddy BV, Suresh V, Nanjunda Rao KS (2016) Characteristic compressive strength of cement-stabilized rammed earth. J Mater Civil Eng 29:04016203

30. Walker P, Stace T (1997) Properties of some cement stabilised compressed earth blocks and mortars. Mater Struct 30(9):545–551

31. Diamond S, Kinter EB (1966) Adsorption of calcium hydroxide by montmorillonite and kaolinite. J Colloid Interface Sci 22(3):240–249

32. Bell FG (1996) Lime stabilization of clay minerals and soils. Eng Geol 42(4):223–237

33. Davidovits J (ed) (2005) Geopolymer, green chemistry and sustainable development solutions: proceedings of the world congress geopolymer 2005. Geopolymer Institute

34. Palomo A, Grutzeck MW, Blanco MT (1999) Alkali-activated fly ashes: a cement for the future. Cem Concr Res 29(8):1323–1329

35. Kebao R, Kagi D, Building Protection TD (2012) Integral admixtures and surface treatments for modern earth buildings. In Modern earth buildings: materials, engineering, constructions and applications, p 256

36. Little B, Morton T (2001) Building with earth in Scotland: innovative design and sustainability. Scottish Executive Central Research Unit, Edinburgh

37. Cheng MY, Saiyouri N (2015) Effect of long-term aggressive environments on the porosity and permeability of granular materials reinforced by nanosilica and sodium silicate. Geotech Eng 46(3):62–72

38. Elert K, Pardo ES, Rodriguez-Navarro C (2015) Alkaline activation as an alternative method for the consolidation of earthen architecture. J Cult Herit 16(4):461–469

39. Slaty F, Khoury H, Rahier H, Wastiels J (2015) Durability of alkali activated cement produced from kaolinitic clay. Appl Clay Sci 104:229–237

40. MOPT (1992) Bases Para el Diseño y Construcción con Tapial. Madrid, Spain: Centro de Publicaciones, Secretaría General Técnica, Ministerio de Obras Públicas y Transportes

41. CRATerre-EAG (1998) CDI, compressed earth blocks: standards—technology series no. 11. CDI, Brussels

42. AFNOR (2001) XP P13-901; Compressed earth blocks for walls and partitions: definitions—Specifications—Test methods—Delivery acceptance conditions

43. Jaquin PA, Augarde CE, Legrand L (2008) Unsaturated characteristics of rammed earth. In: First European conference on unsaturated soils, Durham, England, pp 417–422

44. Beckett CTS, Augarde CE (2012) The effect of humidity and temperature on the compressive strength of rammed earth. In: Proceedings of 2nd european conference on unsaturated soils, pp 287–292

45. AFNOR (1993) NF P 94-051; Soils: Investigation and testing—Determination of Atterberg's limits—Liquid limit test using Casagrande apparatus—Plastic limit test on rolled thread

46. ASTM D2487-11 (2011) Standard practice for classification of soils for engineering purposes. Unified Soil Classification System, USCS

47. Houben H, Guillaud H (1994) Earth construction: a comprehensive guide. Intermediate Technology Publications, London

48. Skempton AW (1953) The colloidal activity of clays. In: Selected papers on soil mechanics, pp 106–118

49. Dierks K, Ziegert C (2002) Neue Untersuchungen zum Materialverhaltenvon Stampflehm. *Steingass, P.: Moderner Lehmbau 2002*

50. Bruno AW (2016) Hygro-mechanical characterisation of hypercompacted earth for building construction. Ph.D. thesis

51. Bruno AW, Gallipoli D, Perlot C, Mendes J (2017) Effect of stabilisation on mechanical properties, moisture buffering and water durability of hypercompacted earth. Constr Build Mater 149:733–740

52. DIN 18945 (2013) Earth blocks—terms and definitions, requirements, test methods

53. Barrett EP, Joyner LG, Halenda PP (1951) The determination of pore volume and area distributions in porous substances. I. Computations from nitrogen isotherms. J Am Chem Soc 73(1):373–380

54. Tarantino A, De Col E (2008) Compaction behaviour of clay. Géotechnique 58(3):199–213

55. Van Jaarsveld JGS, Van Deventer JSJ, Lukey GC (2002) The effect of composition and temperature on the properties of fly ash-and kaolinite-based geopolymers. Chem Eng J 89(1):63–73

56. Innocenzi P, Brusatin G (2004) A comparative FTIR study of thermal and photo-polymerization processes in hybrid sol–gel films. J Non Cryst Solids 333(2):137–142

57. Ciancio D, Beckett CTS, Carraro JAH (2014) Optimum lime content identification for lime-stabilised rammed earth. Constr Build Mater 53:59–65

58. Bruno AW, Gallipoli D, Perlot C, Mendes J (2017) Mechanical behaviour of hypercompacted earth for building construction. Mater Struct 50(2):160

59. Gallipoli D, Gens A, Chen G, D'Onza F (2008) Modelling unsaturated soil behaviour during normal consolidation and at critical state. Comput Geotech 35(6):825–834

60. Gelard D, Fontaine L, Maximilien S, Olagnon C, Laurent J, Houben H, Van Damme H (2007) When physics revisit earth construction: Recent advances in the understanding of the cohesion mechanisms of earthen materials. In: Proceedings of the international symposium on earthen structures, vol. 294302. IIS Bangalore, pp 337–341

61. Jaquin PA, Augarde CE, Gallipoli D, Toll DG (2009) The strength of unstabilised rammed earth materials. Géotechnique 59(5):487–490

62. McGregor F, Heath A, Maskell D, Fabbri A, Morel JC (2016) A review on the buffering capacity of earth building materials. In: Proceedings of the Institution of civil engineers—construction materials. https://doi.org/10.1680/jcoma.15.00035

63. Künzel HM (1995) Simultaneous heat and moisture transport in building components. In: One-and two-dimensional calculation using simple parameters. IRB-Verlag Stuttgart

64. Rode C, Peuhkuri RH, Mortensen LH, Hansen KK, Time B, Gustavsen A et al (2005) Moisture buffering of building materials. Technical University of Denmark, Department of Civil Engineering, Copenhagen